Photoannulation of 4,4-Dimethylcyclohex-2-en-1-one To 1,1-Diphenylethylene

Richard A. Caldwell,* Ralf Constien, and Bryan G. Kriel

Department of Chemistry, The University of Texas at Dallas, Richardson, Texas 75083

Received: July 29, 2002; In Final Form: February 26, 2003

The photoannulation of 4,4-dimethylcyclohex-2-en-1-one (DMC) to 1,1-diphenylethylene (DPE) results in the [2+2] formation of cyclobutanes exhibiting regio- and stereoselectivity. Additionally, regio- and stereoisomers of substituted octahydrophenanthrenes are produced. Formally, these are derived from alpha−ortho coupling of a 1,4-biradical, followed by rearomatization. From laser flash photolysis experiments, we conclude that the temporal absorbance profile observed following excitation of DMC in the presence of DPE is a composite of multiple triplet state transients that includes triplet state 1,1-diphenylethylene and likely includes a triplet state 1,4-biradical. This analysis of the transient data reveals energy transfer and product forming interactions between ^{3}DMC and ground-state DPE. The present work renders our earlier interpretation [*J. Am. Chem. Soc.* **1996**, *118*, 8741],[1] that the transient observed in this system was a ^{3}DMC−DPE exciplex, unnecessary and unlikely.

Introduction

The [2+2] photocycloaddition of α, *β*-unsaturated carbonyl compounds to olefins is well established; in fact, it has been proffered as the most widely used of photosynthetic reactions.[2] This annulation has become the preferred route for the construction of cyclobutane containing compounds and for synthetic strategies that incorporate such structures. The mechanism of this reaction has received considerable study. Initially, Corey proposed a mechanism involving an "oriented *π*-complex" (which now would be called an exciplex) to explain regio- and stereoselectivity in triplet state photocycloadditions of cyclohexenones.[3] Although many subsequent investigations thoroughly documented the existence and the importance of singlet exciplexes in singlet state photocycloadditions, by direct detection, there have been no clear examples of direct detection of exciplexes in triplet state photocycloadditions.

Indirect evidence, however, abounds. Loutfy and de Mayo have rationalized their data for the cycloadditions of ketones to alkenes using an exciplex.[4,5] Exciplexes have been claimed in a number of intramolecular reactions.[6−10] Caldwell has found evidence for exciplexes in the Paterno−Buchi reaction; this was latter supported by the work of Wagner and Winnik.[11−15] Wilson and Halpern have reported exciplex formation between aliphatic ketones and benzene derivatives,[16,17] and Haselbach has presented indirect evidence for an exciplex in quenching experiments using benzophenone.[18]

Alternatively, Bauslaugh has explained the regio and stereoselectivity of ketone−olefin photoannulations on the basis of the stability of the biradical intermediates.[19] Schuster has questioned the need for exciplexes in cyclohexenone photoannulations and supports an interpretation using a biradical model.[20−23] Peters has interpreted the quenching of ketone triplets by electron rich alkenes as direct formation of a biradical.[24,25] Biradical-trapping studies have led Weedon to conclude that exciplexes are not a requirement in explaining the regiochemical outcome of enone−alkene photoannulations.[26−28]

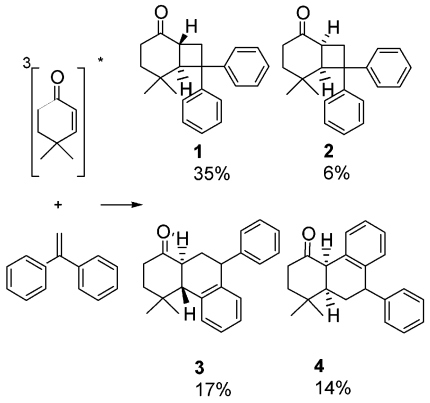

Figure 1. Major products of DMC and DPE photoannulation reaction.

Chapman and Rettig have conducted a prior study of the DMC−DPE photoaddition.[29] This study, conducted in benzene and in tertiary butanol, reports the formation of the trans cyclobutane, **1**, Figure 1. In previous communications, our laboratory has reported on the DMC−DPE annulation in cyclohexane[1] and reported the simultaneous formation of cyclobutanes and octahyrophenanthrenes in the *p*-acetyl styrene−styrene system.[30] The major products of the DMC−DPE annulation are presented in Figure 1. In our initial DMC−DPE study, we concluded that the transient spectroscopy indicated a triplet exciplex intermediate. The study we here describe leads to a different and we now believe more likely interpretation of the transient data, although the existence of a triplet exciplex is not expressly excluded from the reaction. We now believe that the transient temporal profile results from the composite absorbance of ^{3}DMC, ^{3}DPE, and probably at least one precycloaddition 1,4-biradical. The reversibility of the formation of the head-to-tail biradical has been demonstrated by irradiation of the cyclobutanes **1** and **2**. The same species are found as in the photoannulation of DMC and DPE, albeit in different yields.

* To whom correspondence should be addressed. Richard A. Caldwell, M/S FN32, University of Texas at Dallas, P.O. Box 830688, Richardson TX 75083-0688. Phone: 972-883-2516 (menu item 7). Fax: 972-883-6371. E-mail: caldwell@utdallas.edu.

10.1021/jp026635x CCC: $25.00
Published on Web 04/04/2003

Experimental Section

4,4-Dimethylcyclohex-2-en-1-one (DMC) and 1,1-diphenylethylene (DPE) were obtained from Aldrich Chemical and were purified by silica gel column chromatography using hexanes and ethyl acetate, followed by Kugelrohr distillation. UV−vis spectra were obtained with a HP 8450A spectrophotometer and the IR spectra with a Nicolet Avatar 360 FT-IR. Gas chromatography was performed on a Shimadzu GC-14 with flame ionization detection (FID) and on a Finnignan GCQ GC/MS. The methods of ionization used for the mass spectral analysis were electron impact (70 eV), methane, and ammonia chemical ionization. Analytical and semipreparative HPLC separations were performed on a HP 1090 liquid chromatograph with a diode array detector (using 270 and 330 nm detection). The columns used were Lichrosphere (Merck) Si 100, 5 μm (4.0 mm o.d. × 250 mm), and Selectosil (Phenomenex) Si 100, 5 μm (10 mm o.d. × 250 mm). NMR experiments were conducted using a Varian 500 MHz ^{Unity}INOVA spectrometer on $CDCl_3$ solutions containing 0.03% tetramethylsilane. Melting points were obtained with a Hoover capillary melting point apparatus. Galbraith Laboratories (Knoxville, TN) performed the elemental analyses.

Preparative irradiation of 4, 4-dimethylcyclohex-2-en-1-one to 1, 1-diphenyethylene was performed with a solution of DMC (2.45 g, 19.71 mmol) and DPE (7.16 g, 39.72 mmol) in 250 mL of cyclohexane. The solution was irradiated for 24 h using a standard quartz immersion well photochemical reactor with a Hanovia 679A 450W medium pressure mercury lamp. A Corning 3320 uranyl glass filter was added for triplet sensitized irradiations. The solution was deoxygenated and continuously mixed by purging with nitrogen for 30 min before and during the irradiation. After concentrating the reaction mixture to 65 g/L, compound **1** was crystallized at room temperature. The isolated crystals were further purified by crystallization from hexanes. The liquor from the initial crystallization was further concentrated by a factor of 2 and a second crystallization was performed at −10 °C. These crystals were composed of a mixture of compounds **3**, **4**, **5**, and **6**. These compounds were isolated by preparative TLC and by semipreparative HPLC. Compounds **5** and **6** are the result of hydrogen abstraction of compound **3**, resulting in one and two additional unstaturations (respectively) of the newly formed six-member ring.

Compound **2** could not be isolated in sufficient quantity for spectral characterization. Its presence was confirmed in the DMC−DPE reaction mixture by retention time and spectral matching of HPLC and GC/MS experiments. Preparation of a standard of *cis*-5,5-dimethyl-7,7-diphenylbicyclo[4.2.0]octan-2-one, **2**, was performed by adding compound **1** (0.5 mg, 1.64 mmol) to a solution of sodium hydroxide (0.62 g, 15.5 mmol) in 50 mL of methanol with stirring at room temperature for 12 h. The reaction mixture was neutralized with dilute hydrochloric acid and extracted 3 times with dichloromethane (100 mL total volume). Pure **2** was obtained by column chromatography with petroleum ether/10% diethyl ether.

Two aldehydes were also observed in the GC/MS and HPLC analysis but were not isolated. Preparation of standards of 2-(1,1-dimethyl-allyl)-3,3-diphenyl-trans-cyclobutanecarboxaldehyde, **7** and 2-(1,1-dimethyl-allyl)-3,3-diphenyl-cis-cyclobutanecarboxaldehyde, **8**, were performed as follows. Solutions of **1** and **2**, respectively, (100 mg, 0.32 mmol in 10 mL cyclohexane) were irradiated in a quartz microscale photochemical reaction assembly with a mercury lamp at a principal output of 254 nm.[31] The reaction mixtures were evaporated and diluted in diethyl ether. The aldehydes **7** and **8** were isolated by preparative TLC (silica, petroleum ether/10% diethyl ether).

Laser flash photolysis experiments were conducted as previously described with Mode-Locking and Q-Switched Continuum Nd:YAG lasers, model Y6571C-10.[32] An Osram model XBO 150 W/I high-pressure xenon lamp and CVI Digikrom 240 monochromator and photomultiplier provided detection. Data were collected using a Tektronix DSA 602 digitizing signal analyzer and transferred to a DTK 486DX personal computer for analysis. Laser and flash lamp control and the kinetic analyses were performed with the PC RAD software package from Kinetic Instruments (Austin, TX). The experiments, unless otherwise noted, were conducted in cyclohexane at room temperature in a 5 × 10 mm quartz cuvette. The full-widths-at-half-maximum height for the mode locked and Q-switched laser pulses were 1.6 and 5 ns, respectively. The mode-locked laser was used when the full temporal profile was to be fitted.[33] The Q-switch laser was used when fitting only the transient signal decay and also to collect time-resolved absorption spectra.[34] Figures 4, 6, 8, and 9 exhibit a feature at 50 ns that is attributed to a cable ring in the laser flash photolysis equipment. For elevated temperature studies, the cuvette was placed in a brass block fitted with resistive heating elements. Dodecane and hexadecane were used as solvents for experiments conducted at elevated temperatures.

The following laser wavelengths, nominal energies, and analytical wavelengths were used for the kinetic studies: ^{3}DMC (355 nm, 5 mJ, 300 nm); ^{3}DPE, sensitized by thioxanthone (355 nm, 5 mJ, 335 nm); head-to-tail ^{3}biradical, by decomposition of **1** and **2** (266 nm, 10 mJ, 335 nm); DMC-DPE temporal profile, resulting from quenching of ^{3}DMC by DPE (355 nm, 15 mJ, 335 nm). Time-resolved spectroscopy was conducted on these transients under the same experimental conditions. The analytical wavelength varied between 300 and 370 nm. Measurement of the quenching rate constant for the energy transfer of the ^{3}thioxanthone−DPE experiment was performed with procedures that were previously described.[35] The quenching rate constant for the ^{3}DMC−DPE system was measured similarly; however; the pseudo-first-order rate constants for the sensitizer were determined using two kinetic models, vide infra. A DMC concentration of 79 mmol, $OD^{355\ nm} = 1.0\ cm^{-1}$, and DPE concentrations between 0 and 0.8 mmol were used in the DMC−DPE quenching experiments.

The transient signal modeling of the laser flash photolysis studies was performed using two kinetic models. Both models employ the method of finite differences.[36] The mode locked laser pulse, as detected by the monochronomator, was used to generate the ERF for iterative reconvolution. Simulations modeled either the first-order sequential two-reaction scheme describing the formation of an exciplex or a composite signal of two first-order decays. The composite model was used to describe two competing interactions of DMC and DPE. Validation of the simulators was performed by demonstrating their ability to fit exact expressions of the respective kinetic model. The simulators were written in Microsoft Excel workbook files using the Solver add-in. The Microsoft Excel Solver uses a generalized reduced gradient (GRG2) nonlinear optimization code. Linear and integer problems use the simplex method with bounds on the variables and the branch-and-bound method.[37] Fitting was performed by minimization of the sum-of-squares of the residues of the differences between the simulated and the experimental data. The sum-of-squares was performed at one-half nanosecond increments.

Results

Preparative photoaddition of DMC to DPE resulted in a mixture of products (Figure 1). The major products were compounds **1**, **2**, **3**, and **4** (35, 6, 17, and 14 wt %, respectively). Another 19% of the material balance is accounted for by six isomers of **3** and **4**, none greater than 5 wt %. Compounds **5** and **6,** resulting from hydrogen extraction of **3**, represent 4% of the material balance, 2% each. Four percent of the balance was comprised of **7** and **8**, approximately two percent each.

The irradiation of **1** afforded the aldehyde **7** as the major product with small amounts of DMC and DPE. The irradiation of **2** resulted primarily in DMC and DPE, with compound **8** as a minor product. The GC/MS analyses of these reactions indicate that compounds **1**−**6** were present in varying amounts for both reactions.

Spectroscopic Data. *trans*-5,5-Dimethyl-7,7-diphenylbicyclo-[4.2.0]octan-2-one, **1**: white crystals (1.81 g, 35.3%) mp 167−168 °C; ^{1}H NMR δ 0.34 (3H, s), 1.25 (3H, s), 1.68−1.74 (1H, ddd), 1.78−1.88 (1H, dt), 2.08−2.14 (1H, ddt), 2.28−2.34 (1H, m), 2.34−2.42 (1H, t), 2.90−2.94 (1H, d, $J_{3.39-3.45}$ = 13.7 Hz), 2.94−3.0 (1H, dd), 3.39−3.45 (1H, m), 7.14−7.30 (10H, m); ^{13}C NMR δ 18.41, 18.47, 28.68, 34.42, 34.84, 38.10, 42.38, 46.85, 56.84, 60.43, 125.67, 126.40, 128.12, 128.16, 128.41, 141.82, 150.17, 209.67; MS (EI, 70 eV) *m*/*z* 304 (M^+, 2), 248 (15), 180 (100), 165 (41). Anal.Calcd for $C_{22}H_{24}O$: C, 86.80; H, 7.95; O, 5.26. Found: C, 87.25 H, 7.96 O, 4.79. HREI MW Calcd: 304.1824, Found: 304.1824.

cis-5,5-Dimethyl-7,7-diphenylbicyclo[4.2.0]octan-2-one, **2**: clear crystals (0.34 g, 6.6%) mp 83−84 °C; ^{1}H NMR δ 0.90−0.96 (1H, ddd), 1.03−1.06 (3H, s), 1.11−1.08 (3H, s), 1.08−1.34 (1H, m), 2.17−2.23 (1H, m), 2.29−2.37 (1H, m) 2.58−2.65m (1H, dd), 2.86−2.92 (1H, dt), 3.33−3.38 (1H, dd), 3.51−3.55 (1H, d, $J_{2.86-2.92}$ = 8.3), 7.16−7.30 (10H, m); ^{13}C NMR δ 26.15, 29.47, 31.94, 33.67, 36.79, 37.00, 40.58, 53.59, 55.89, 125.55, 126.14, 126.62, 127.62, 128.11, 129.77, 142.31, 152.19, 215.85; MS (EI, 70 eV) *m*/*z* 304 (M^+, 3), 248 (15), 180 (100), 165 (44). Anal.Calcd for $C_{22}H_{24}O$: C, 86.80; H, 7.95; O, 5.26., HREI MW Calcd: 304.1824, Found: 304.1835.

1-Keto-4,4-dimethyl-9-*cis*-phenyl-1,2,3,4,4a,9,10-*trans*-10a-octahydrophen-anthrene, **3**: white crystals (0.85 g, 17%) mp 164−165 °C; ^{1}H NMR δ 1.00 (3H, s), 1.69 (3H, s), 1.64−1.78 (2H, m), 1.92−2.10 (1H, dt), 2.28−2.46 (3H, m), 2.55−2.58 (1H, dt), 2.85−2.9 (1H, d, $J_{2.55-2.58}$ = 12.67 Hz), 4.4−4.8 (1H, dd, $J_{2.55-2.58}$ = 2 Hz, $J_{2.28-2.46}$ = 1 Hz), 7.0−7.24 (8H, m), 7.62−7.64 (1H, d); ^{13}C NMR δ 23.66, 29.13, 32.06, 35.06, 35.21, 36.32, 40.19, 42.12, 43.94, 48.71, 125.92, 126.06, 126.09, 128.11, 128.86, 131.02, 138.40, 139.81, 145.27, 213.77; MS (EI, 70 eV) *m*/*z* 304 (M^+, 7), 286 (3), 248 (100), 233 (18), 205 (31). Anal. Calcd for $C_{22}H_{24}O$: C, 86.80; H, 7.95; O, 5.26. Found: C, 87.33; H, 7.95; O, 4.72; HREI MW Calcd: 304.1824, Found: 304.1831.

4-Keto-1,1-dimethyl-9-*cis*-phenyl-1,2,3,4,4a,9,10-*cis*-10a-octahydrophenanthrene, **4**: white crystals, (0.70 g, 14%) mp 114−115 °C; ^{1}H NMR δ 0.80 (3H, s), 1.32 (3H, s), 1.62−1.69 (1H, m), 1.78−1.85 (2H, m), 1.95−2.02 (1H, m), 2.02−2.1 (1H, m), 2.32−2.40 (1H, m), 2.60−2.68 (1H, dd), 3.95−4.05 (1H, d, $J_{2.02-2.1}$ = 1.8 Hz), 4.30−4.38 (1H, dd, $J_{1.78-1.85}$ = 1.8 Hz, $J_{1.95-2.02}$ <1 Hz), 6.95−7.15 (9H, m); ^{13}C NMR δ 26.95, 27.84, 30.59, 32.52, 35.47, 38.24, 42.67, 43.87, 52.49, 125.88, 127.12, 128.00, 128.69, 129.18, 130.66, 131.27, 134.42, 137.61, 147.33, 210.90; MS (EI, 70 eV) *m*/*z* 304 (M^+, 97), 286 (18), 271 (22), 245 (30), 233 (88), 204 (100), HREI MW Calcd: 304.1824, Found: 304.1829.

TABLE 1: X-ray Structure Data of the Cyclobutane 1 and Octahydrophenanthrene 3

	compound **1**	compound **3**
formula	$O_1C_{22}H_{24}$	$O_1C_{22}H_{24}$
formula wt.	304.44	304.44
crystal system	monoclinic	monoclinic
space group	*P*21/*N* (no. 14)	*P*21/*C* (no. 14)
color	clear	clear
unit cell: *a*,*b*,*c* Å	11.251,10.884, 14.336	8.684,9.567, 19.776
Z	4	4
R	0.0453	0.0388
R_W	0.0456	0.0376
GOF	1.168	0.745
LinAbs.Coeff.	0.0645	0.0685
temp. °C	23	23
wavelength of rad.(λ, Å)	Mo Kα (0.71069)	Mo Kα (0.71073)
2θ range	4° ≤ 2θ≤50°	4° ≤ 2θ≤50°
number of data & cutoff	1073 & 3	1658 & 3
parameters refined	280	304
calculated density g/mL	1.157	1.235
intensity measure	ω−2θ,scan	ω−2θ,scan

1-Keto-4,4-dimethyl-9-phenyl-1,2,3,4,4a,-*trans*-10a-hexahydrophenanthrene, **5**: white crystals, (0.10 g, 2%) mp 126−127 °C; ^{1}H NMR δ 1.532 (3H, s), 1.537 (3H, s), 1.82−1.84 (1H, m), 1.84−1.86 (1H, d), 2.35−2.75 (1H, t), 2.45−2.46 (1H, t), 2.63−2.67 (1H, t), 2.67−2.72 (1H, t), 2.95−3.05 (1H, d), 3.11−3.18 (1H, dd), 6.73−6.75 (1H, d), 7.05−7.38 (8H, m), 7.79−7.82 (1H, d); ^{13}C NMR δ 19.37, 29.69, 30.30, 32.56, 37.61, 43.73, 47.23, 51.51, 125.76, 126.00, 126.57, 126.71, 127.34, 128.21, 128.71, 137.00, 137.08, 139.66, 140.06, 208.21; MS (EI, 70 eV) *m*/*z* 302 (M^+, 41), 285 (6.3), 246 (19), 231 (8), 204 (100), HREI MW Calcd: 302.1668, Found: 302.1676.

1-Keto-4,4-dimethyl-9-phenyl-1,2,3,4a-tetrahydrophenanthrene, **6**: white crystals, (0.11 g, 2%); UV−vis $\epsilon_{Max}^{339} = \epsilon_{Max}^{355}$ = 835 cm^{-1} mol^{-1} L (cyclohexane); ^{1}H NMR δ 1.84 (6H, s), 2.08−2.22 (2H, m), 2.78−2.82 (2H, m), 7.4−7.9 (10H, m); ^{13}C NMR δ 13.9, 26.7, 34.39, 41.05, 124.09,125.04, 127.4, 128.99, 127.21, 128.27, 129.46, 130.03, 131.03, 131.67, 135.46, 138.62, 139.56, 140.20, 149.35; MS (EI, 70 eV) *m*/*z* 300 (M^+, 81), 285 (100), 270 (4), 267 (5), 257 (52). HREI MW Calcd: 300.1512, Found: 300.1516.

2-(1,1-Dimethyl-allyl)-3,3-diphenyl-cyclobutanecarbaldehyde, **7**: oil, (15 mg,); ^{1}H NMR δ 0.70 (3H, s), 0.79 (3H, s), 2.31−2.43 (1H, m), 2.90−3.09 (1H, m), 3.39 (2H, dd), 4.68−4.79 (2H, m)5.40 (1H, dd), 9.66 (s,1H), ^{13}C NMR δ 25.2, 33.5, 39.6, 44.6, 53.2, 53.5, 112.0, 125.9, 126.8, 127.0, 127.6, 129.8, 143.8, 145.4, 151.5, 203.1; MS (EI, 70 eV) *m*/*z* 304 (M^+, 1), 205 (5), 180 (100), 165 (61), 152 (4), 129 (5), 115 (11), 91 (10). IR (KBr): 1766 cm^{-1} (C═O).

The X-ray structure of *trans*-5,5-dimethyl-7,7-diphenylbicyclo[4.2.0]-octan-2-one **1** and **4**, 4-dimethyl-9-phenyl-3,4,-4a,9,10,10a-hexahydro-2*H*-phenanthren-1-one, **3**, were determined, see Table 1 and Figure 2. The preliminary examination and data collection were accomplished using an Enraf-Nonius CAD4 diffractometer. Cell constants were obtained by a least-squares fit of 25 reflections. The space groups of the monoclinic cells were determined to be $P2_1/n$ (no 14) for compound **1** and $2_1/C$ (no 14) for compound **3**. The structures were solved by direct methods and refined on the basis of 1073 observed reflections for **1** and 1658 observed reflections for **3**. Hydrogen atoms were calculated at idealized positions and included in the calculations but not refined. Least-squares refinement was conducted in the range of 4.00° < 2θ < 50.0° and converged at $R_{(1)}$ = 0.0453, $R_{(3)}$ = 0.0388, and $R_{w(1)}$ = 0.0456, $R_{w(3)}$ = 0.0376.

The literature values for the lifetimes and the λ_{max} of ^{3}DMC and ^{3}DPE were reproduced. ^{3}DMC, generated by direct excita-

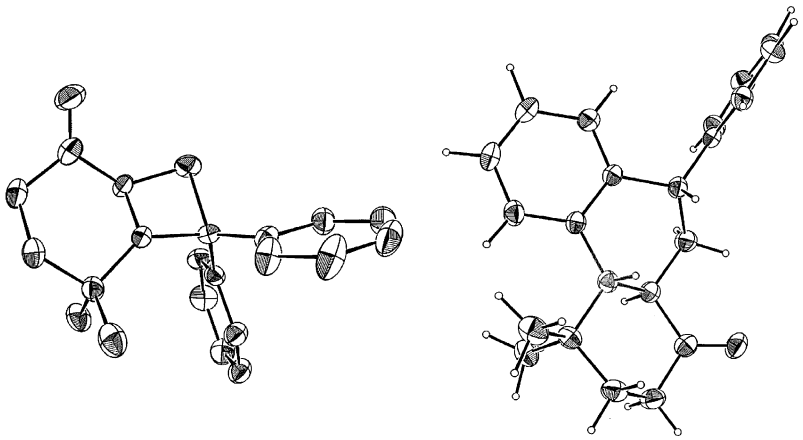

Figure 2. Thermal ellipsoid plot of the head-to-tail *trans*-cyclobutane, compound **1**, and the head-to-tail *trans*-octahydrophenanthrene, compound **3**.

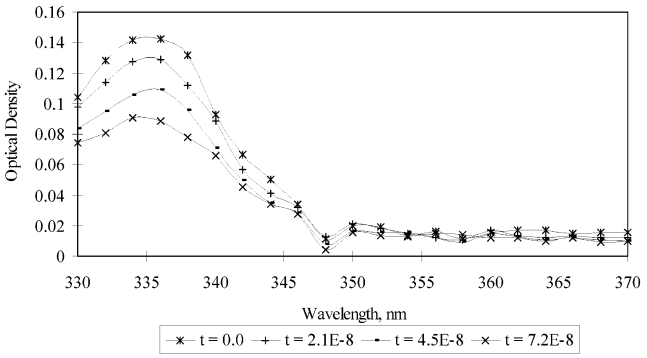

Figure 3. Time-resolved absorption spectrum for the head-to-tail ^{3}-[biradical] formed by irradiation of the cyclobutane **1**, $\lambda_{max} = 335$ nm.

tion at 355 nm, exhibits an absorption spectrum with a λ_{max} of 295 nm and decays with a lifetime of $\tau = 24 \pm 1$ ns. ^{3}DPE, generated by energy transfer from thioxanthone, has a λ_{max} of 335 nm and a lifetime of $\tau = 36 \pm 1$ ns. The time-resolved spectrum for the head-to-tail ^{3}biradical generated by photolysis of **1** is presented in Figure 3 and has $\lambda_{max} = 335$ nm and a lifetime of $\tau = 36 \pm 1$ ns. A similar spectrum was obtained by the photolysis of **2**. The temporal profile for the head-to-tail ^{3}biradical generated by photolysis of either **1** or **2** resulted in a 78 ns transient. The laser flash photolysis of **1** is presented in Figure 4. Irradiation of **1** results in **7** as the major product, and irradiation of **2** results in DPE and DMC as major products. The photolysis of **2** resulted in a similar temporal profile with the same first-order lifetime of 78 ± 2 ns. The time-resolved spectrum for DMC−DPE laser flash photolysis experiment has a λ_{max} of 337 nm, Figure 5. A first-order fit of the DMC−DPE temporal profile at 335 nm results in a lifetime of $\tau = 49$ ns, Figure 6, which could be used to infer a new species. However, the measured first-order lifetime of the DMC−DPE temporal profile is dependent on the analytical wavelength, Figure 7, vide infra.

The DMC−DPE temporal data of Figure 6 was also fitted using two kinetic models. In Figure 8, the fit using the exciplex model (first-order sequential, two reaction kinetics) resulted in a lifetime of $\tau = 48$ ns, which is a reasonable agreement with the first-order fit. Because a small permanent absorbance was observed, a correction was applied by assuming that it resulted from decay of the exciplex and that its magnitude was proportional to the extent of decay. The DMC−DPE temporal profile was also fitted using a model in which two first-order transients contribute to yield a composite signal. The lifetime of the first transient was constrained to 36 ns (the lifetime of ^{3}DPE) and the lifetime of the second transient was constrained to 78 ns (the lifetime of the ^{3}[biradical]). As seen in Figure 9, this also resulted in a good fit of the DMC-DPE temporal profile.

Quenching experiments were conducted in order to determine k_q, the quenching rate constant, using the relationship $k_{obs} = k_d{}^3\text{DMC} + k_q[\text{Q}]$. Here, k_{obs} is the observed quenching rate, and it is dependent on the quencher concentration [Q]. The rate of decay of triplet state DMC is $k_d{}^3$DMC, and k_q is the quenching rate constant. Before fitting the data, a signal correction was performed for the ^{3}DMC signal. The ^{3}DMC correction was calculated using the rate constant for ^{3}DMC quenching by DPE (determined iteratively) and the ^{3}DMC signal amplitude-to-laser power ratio, which was used to scale the amplitude of the correction. The corrected data was then fitted using the exciplex model and the composite model, Figure 10. The quenching curve for the exciplex model yields $k_d{}^3\text{DMC} = 4.91 \times 10^7\ \text{s}^{-1}$. The quenching curve for the composite model yields $k_d{}^3\text{DMC} = 4.07 \times 10^7\ \text{s}^{-1}$. The independently measured (and literature) value of $k_d{}^3$DMC is $1/\tau = 4.17 \times 10^7\ \text{s}^{-1}$ is noted in Figure 10. Using the composite model, an Arrhenius plot was generated within a temperature range of 25 to 150 °C with five temperature stations. Cyclohexane, dodecane, and hexadecane were used as solvents. Overlap experiments were performed at the transition temperatures, and in all cases, these resulted in comparable results for both solvents. The activation energy for the quenching of ^{3}DMC by DPE was measured to be 1.1 kcal/mol. The rate constant is significantly slower than that for a diffusion-limited event, as is known to be the case for excitation transfer from nonvertical donors, and the activation energy is lower than that expected for diffusion.[11] There is no requirement that the activation energy exceed that for diffusion in such a case, because the quenching act involves both formation and separation of reactant contact pairs, and diffusive control operates in both diretions.

Discussion

Compounds **1** and **2** exhibit *retro*-[2+2] mass spectral fragmentation, with a low intensity molecular ion (304 amu) and a base ion at $m/z = 180$ (MW of DPE). In the ^{1}H NMR spectrum, **1** is best distinguished by the upfield proton shift at $\delta = 0.34$ ppm. This shift is due to a phenyl ring affect. The trans isomer is evidenced by the bridging methine's axial−axial coupling constant of 13.7 Hz. Compound **2** exhibits chemical

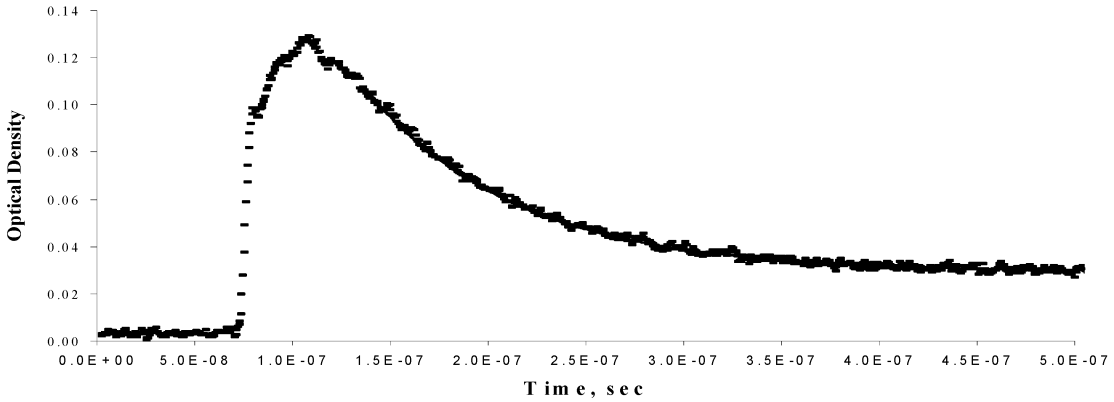

Figure 4. Temporal curve depicting first-order decay of the head-to-tail ^{3}[biradical] formed by irradiation of the cyclobutane **1**, $\tau = 78 \pm 2$ ns, measured at 335 nm, 27 °C.

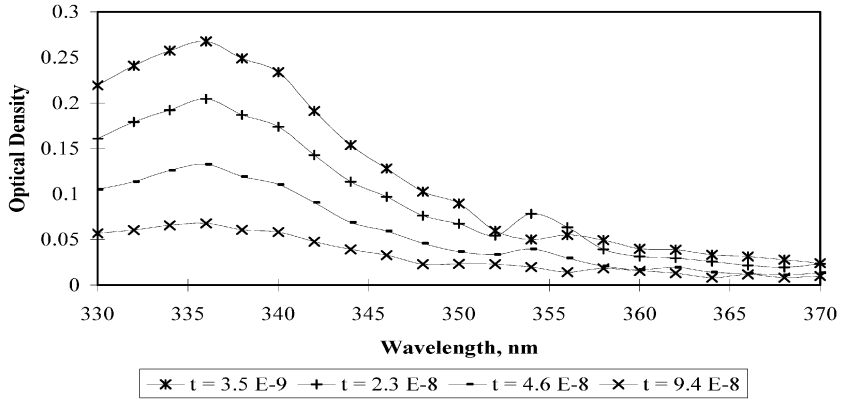

Figure 5. Time-resolved absorption spectrum for the DMC−DPE temporal signal, $\lambda_{max} = 337$ nm.

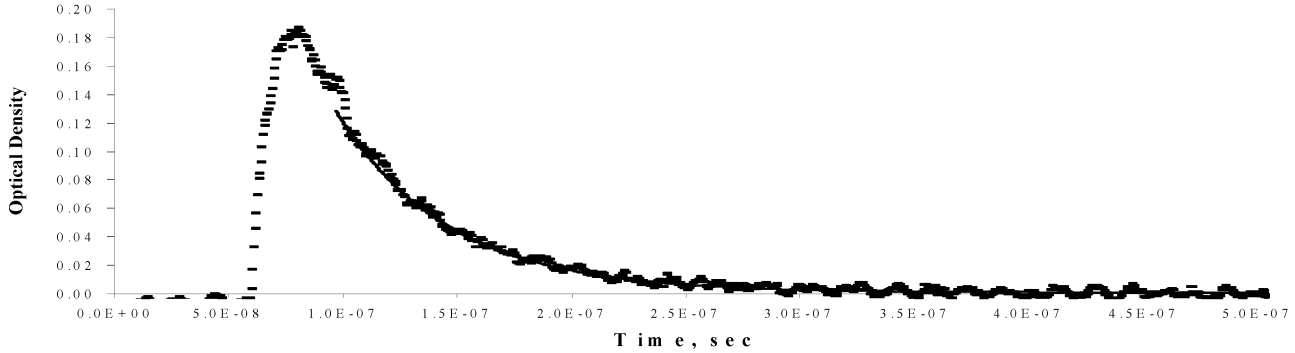

Figure 6. First-order decay of the DMC−DPE temporal profile, $\tau = 49 \pm 0.5$ ns, measured at 335 nm, 27 °C. [DPE] = 0.7 M.

shifts of the beta hydrogens in the cyclohexane spin system at $\delta = 0.94$ and 1.05 ppm because of shielding by the phenyl group that is trans to the ring junction methines. The bridging methine hydrogens of **2** possess a relatively large coupling constant of 8.3 Hz due to the small dihedral angle. The mass spectrum of compound **3** reflects the head-to-tail regiochemistry. The base ion at $m/z = 248$ amu exhibits enolization followed by a *retro*-Diels−Alder fragmentation, expected for the head-to-tail isomer but not the head-to-head isomer.[38] The stereochemistry of compound **3** is trans, as determined by the methine coupling constant of 12.7 Hz. The stereochemistry of the benzylic hydrogen, with respect to the methine hydrogen α to the carbonyl is also trans, this is determined by the coupling constants of 1−2 Hz with its vicinal hydrogens. These coupling constants define the hydrogen position as pseudoequatorial and the phenyl group as axial. The dominant mass spectral ion fragment of compound **4** is at $m/z = 204$ amu; this is the 1-phenylnaphthalene radical cation. In the ^{1}H NMR, the bridging methine stereochemistry is cis with respect to the methine hydrogens. This is determined from the methine coupling constant of 1.8 Hz. The benzylic hydrogen is in an equatorial position, as seen by the associated coupling constants of 1.8 and less than 1.0 Hz. The phenyl group is pseudoaxial and cis with respect to the methine hydrogen. Compound **5** exhibits an additional unsaturation with respect to the 1:1 adducts ($M^+ = 302$ amu) and head-to-tail regiochemistry, again displaying the retro-Diels−Alder fragmentation observed with compound **3** ($m/z = 246$ amu). Reasonable agreement with the calculated olefinic hydrogen shift $\delta = 6.4$ ppm with the observed shift of $\delta = 6.6$ ppm support the assignment of the additional unsaturation. The phenanthrene, **6**, exhibits two additional unsaturations with respect to compound **3** ($M^+ = 300$ amu). The large intensity of the molecular ion and the m-15 ion ($m/z = 285$) indicate development of new aromaticity.

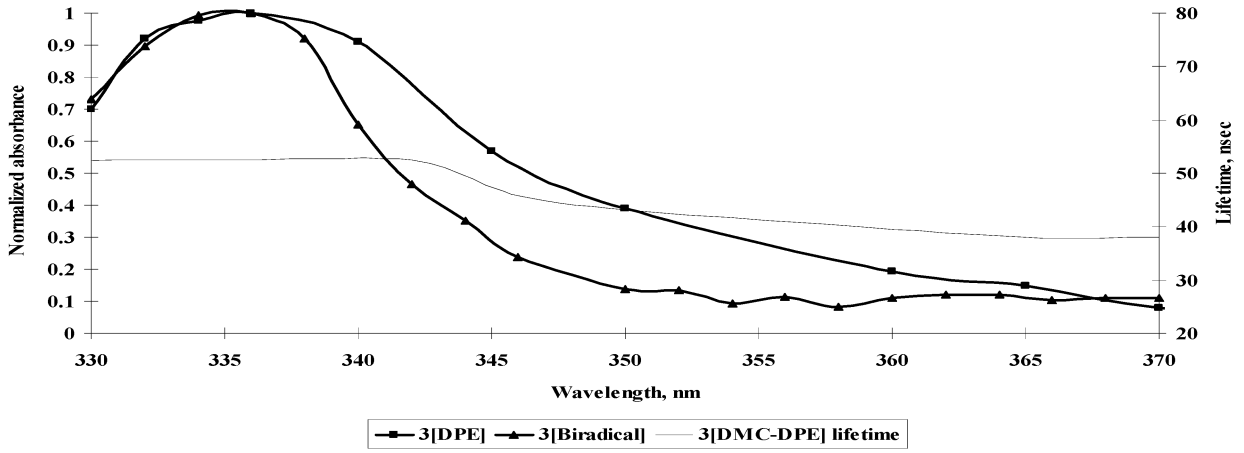

Figure 7. Dependence of the DMC−DPE transient signal lifetime on the analytical wavelength.

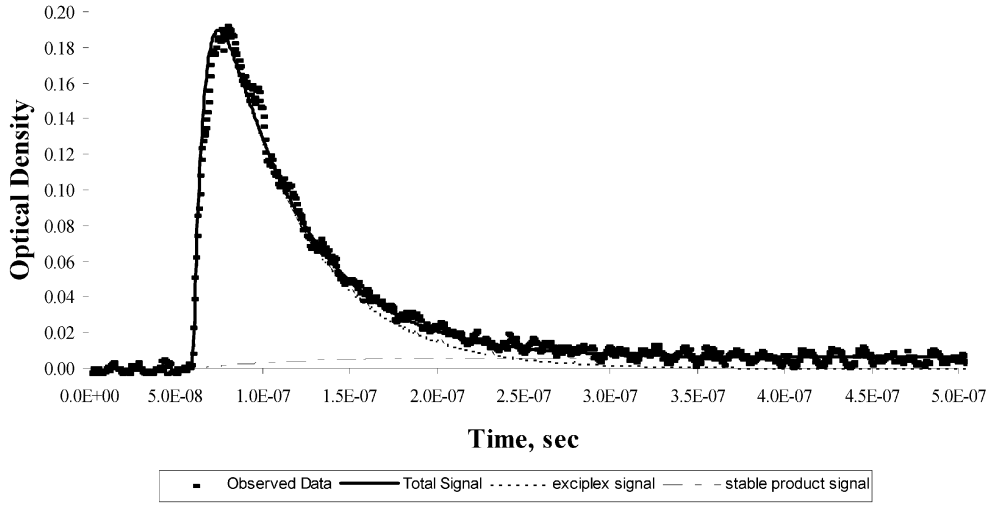

Figure 8. Temporal curve depicting the fit for the first-order sequential two reaction exciplex model for the DMC−DPE temporal profile, $\tau = 48 \pm 2$ ns.

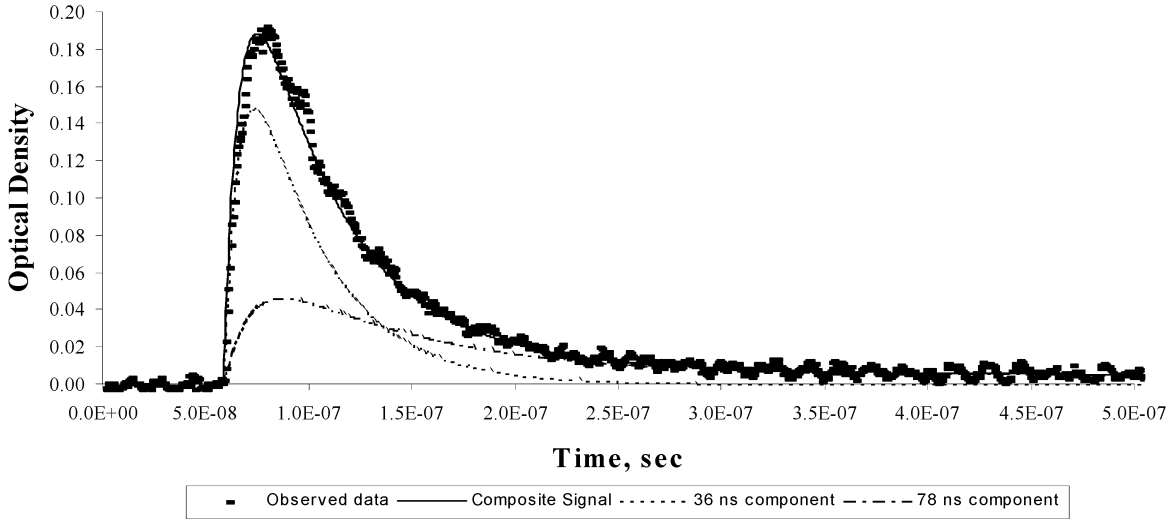

Figure 9. Temporal curve depicting the composite signal fit for the DMC−DPE temporal profile, $\tau_1 = 36$, $\tau_2 = 78$ ns.

There are three elementary experiments that may be used to determine whether laser flash photolysis has produced a single transient. First, time-resolved spectra should be, except for amplitude, identical at all times. Second, the natural log of the decay of the temporal curve should yield a straight line at all wavelengths. Third, the first-order lifetime of the temporal profile must be invariant over a wide range of wavelengths. For a temporal profile composed of multiple transients, the first-

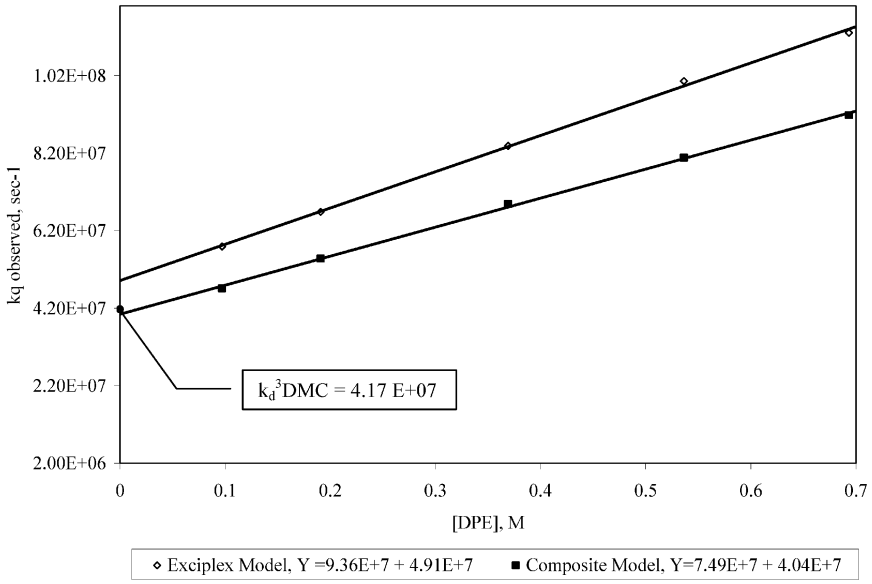

Figure 10. Quenching crves generated by the first-order sequential two reaction model and by the composite ^{3}DPE and head-to-tail ^{3}biradical model.

order lifetime is a function of the extinction coefficients and the concentrations of the species in the system: $OD^t_\lambda = \sum_{i=1}^{n} \epsilon^i_\lambda c_0 e^{-k^i(t)}$. If the lifetimes and extinction coefficients of the transients significantly differ, time-resolved spectra may vary with time, logarithmic plots of decay may be nonlinear, and the apparent (best-fit) first-order decay rate constant may vary with wavelength.

We compare the present results to our first DMC−DPE laser flash photolysis study.[1] It is clear from the comparison that such variations may be small enough that the experimental outcomes can be misinterpreted. The DMC−DPE time-resolved spectra in Figure 3 are acceptably uniform, consistent with a single transient species. Note, however, that multiple transients each possessing similar spectra may also generate spectra uniform enough to lead to an unwarranted conclusion of a single transient. The natural log of the DMC−DPE temporal profile in Figure 6 appears to be a straight line at normal laser energies because of poor signal-to-noise late in the decay. Repeating this experiment at higher high laser energy, i.e., at better signal-to-noise, we can discern a small curvature. In the third test, at normal laser energies, the first-order lifetime of the DMC−DPE temporal profile was a constant 49 ns, over the region were sufficient absorbance could be measured. This experiment was also repeated using higher laser energy (21 mJ, focused), and the dependence of the lifetime on the analytical wavelength became evident (Figure 7). This is further evidence of the presence of more than one transient species. The lifetime has a maximum of 49 ns over a range from 330 to 343 nm and a minimum value of 38 ns at 365 nm. The 38 ns lifetime is indicative of the presence of ^{3}DPE, which has a 36 ns lifetime. We now conclude that a single transient is insufficient to explain all of the kinetic results.

From the new information, we assign, as well as possible, the transients that are present. First, the shorter lived of the two transients is likely to be ^{3}DPE, because the 38 ns lifetime is observed in the spectral region where ^{3}DPE is expected to afford the dominant absorbance. Second, at least one transient in the composite has a lifetime significantly greater than 38 ns. Third, the ratio of the extinction coefficients of the transients must be relatively constant in the 330−343 nm region. The head-to-tail ^{3}[biradical], cf. Figures 4 and 7, which is the precursor of the major product, possesses the characteristics of, and we believe may well be, the long-lived transient. We expect little variation of triplet 1,4-biradical lifetime with structure (i.e., head-to-tail or head-to-head), so we must not rule out isomeric biradicals. Indeed Weedon[39] has shown that biradical yields may be poorly predicted from product yields.

To test this biradical hypothesis, the composite model (^{3}DPE, $\tau_1 = 36$ ns and head-to-tail ^{3}[biradical], $\tau_2 = 78$ ns) was used to fit the DMC−DPE temporal profile. As seen in Figure 9, the two signals can be combined to fit the DMC−DPE temporal profile. However, the fit by the exciplex model is comparable; Figure 8. No conclusive decision can be made based on the fit alone. From the regression of the quenching data, Figure 10, the predicted rate of decay of ^{3}DMC by the composite model is $(4.04 \pm 0.1) \times 10^7$ s^{-1}, a three percent error as compared to the known rate of decay. The regression for the exciplex model is $4.91 \pm 0.1 \times 10^7$ s^{-1}, a seventeen percent error in the prediction of the rate of thermal decay of ^{3}DMC. Clearly, the composite model is in better agreement with the known rate of decay of ^{3}DMC. In summation, the curvature of the natural log of the temporal profile, the dependence of the first-order lifetime on wavelength, and the accuracy of the composite model's quenching curve are strong arguments that the observed DMC−DPE temporal profile is (primarily) the result of ^{3}DPE and the absorbance of a longer-lived species which we expect to be the head-to-tail ^{3}[biradical]. Other transient species may be present; however, they are either minor contributors or they closely mimic one of these two transients.

The composite ^{3}DPE and ^{3}biradical transient argument can be used to interpret the oxygen and azulene quenching experiments presented in our earlier communication.[1] The production of singlet oxygen by the DMC−DPE system was undertaken in aerated cyclohexane. S_Δ values for the production of singlet oxygen by DMC ($OD_{355} = 1.0$; $\Phi_T = 1.0$) and DPE (sensitized by p-methoxyacetophenone, $OD_{355} = 1.0$) were determined to be 0.55 and 0.19, respectively.[40] The Φ_Δ for a solution of DMC ($OD_{355} = 1.0$) and DPE (0.4M) can be predicted from the DMC and DPE triplet lifetimes, the rate at which the enone triplet is quenched by DPE (7.5×10^7 L mol^{-1} s^{-1}), the oxygen quenching rates (^{3}DMC $= 4.6 \times 10^9$ L mol^{-1} s^{-1}, ^{3}DPE $= 6.3 \times 10^9$ L mol^{-1} s^{-1}) and the S_Δ for the oxygen quenching events.

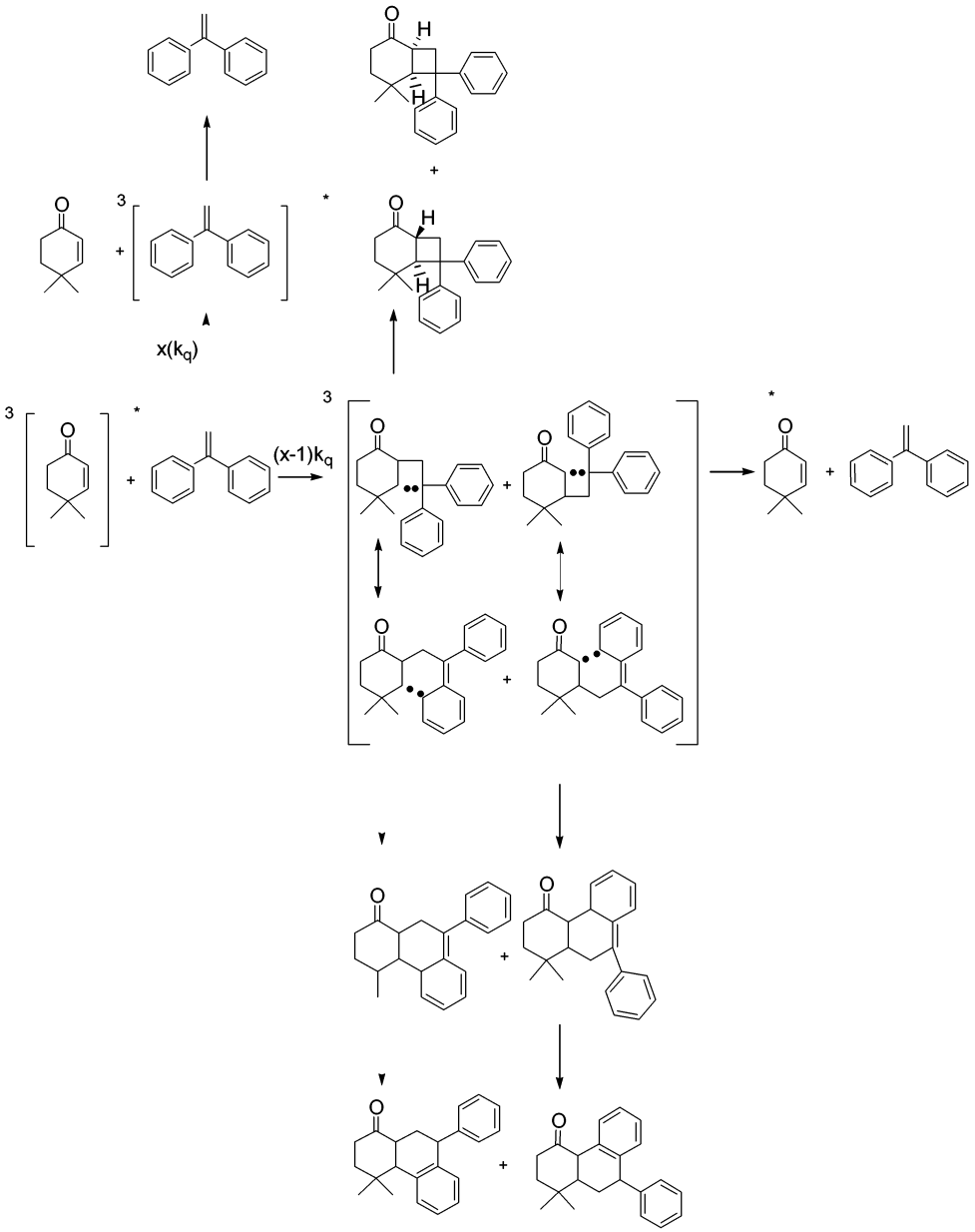

Figure 11. Reaction scheme for DMC−DPE interactions involving energy transfer, 1,4 annulation, and 1,6 annulation.

If the interaction between the enone triplet and DPE produced DPE triplets exclusively, the predicted Φ_Δ would be 0.092 ± 0.004, which is greater than the observation of 0.080 ± 0.004. The contribution due to quenching of ^{3}DMC is predicted to be 0.069. From this, we conclude that there is modestly more singlet oxygen formed than may be explained by ^{3}DMC−O_2 quenching alone. We attribute the excess to ^{3}DPE−O_2 quenching, further supporting the presence of ^{3}DPE. That the observed Φ_Δ of 0.080 is between the predicted extremes of complete energy transfer and no energy transfer is indicative that some ^{3}DMC−DPE interactions do not result in ^{3}DPE formation (as is clear regardless from the formation of the cycloadducts). From this analysis, we estimate the yield of ^{3}DPE from the ^{3}DMC−DPE interactions to be 58 ± 18%. A similar result is obtained from a very different approach. In composite transient modeling, the ^{3}DPE curve is responsible for approximately 56% of the composite signal, as determined from the intensities of the ^{3}[biradical] and ^{3}DPE absorbance profiles in Figure 9, assuming their extinction coefficients are of similar magnitude. As a result of these treatments, we suggest that the ^{3}DMC−DPE interactions partition about one to one between energy transfer and biradical formation channels.

In the azulene quenching experiments, quenching of ^{3}DMC by DPE with a rate constant of 7.5×10^7 L mol^{-1} s^{-1} leads to a predicted Φ_{3AZ^*}(DPE)/Φ_{3AZ^*} of 0.44 (the ratio of the azulene triplet in the presence and absence of DPE).[1] This is to be compared with the measured Φ_{3AZ^*}(DPE)/Φ_{3AZ^*} value of 0.47. The reasonable agreement between the predicted and observed values indicates that the predominant, and probably the only, source of ^{3}azulene is ^{3}DMC. ^{3}DPE is known[41] not to transfer energy to azulene, and thus the most reasonable source of ^{3}-azulene is ^{3}DMC. ^{3}DMC can generate ^{3}DPE by energy transfer. The energy transfer is exothermic by 11.5 kcal/mol (DMC − $E_{T(rel)}$ 63 ± 0.7; DPE − $E_{T(spec)}$ 60.8, $E_{T(rel)}$ 52.1 ± 1.8 kcal mol^{-1}). We have considered that ^{3}DPE could be generated by a Schenck-like mechanism. However, this involves an endothermic step (conversion of the Schenck biradical to ^{3}DPE and

DMC) with an enthalpy of approximately 7.7 kcal/mol, as estimated by Benson calculations.[42,43]

It is notable that we observed no head-to-head cyclobutanes. We conclude that they are formed in at most very low yield. The head-to-tail biradical has been observed, by photolysis of **1** and **2**, with a measured lifetime of 78 ns. The presence of at least one 78 ns transient with λ_{max} ca. 335 nm is consistent with our analysis of the DMC−DPE quenching experiments. The formation of compound **4** may be evidence for the existence of a head-to-head ^{3}biradical, a possibility we are currently investigating. The presence of a six-member ring head-to-head product leads us to believe that it is the failure of ring closure that prevents the formation of the cyclobutane regio-isomers. We have at present no convincing explanation for the absence of head-to-head products.

The hypothesis that the head-to-tail ^{3}biradical is common to both the DMC−DPE photocycloaddition and the photofragmentation of **1** and **2** places constraints on the products in the two directions. Our observation that photolysis of either **1** or **2** produces DMC and DPE is consistent with this hypothesis. Because aldehydes are only observed in the photolysis of either **1** or **2** and not in the photocycloaddition direction, we believe they must arise by a pathway unavailable in the photocycloaddition direction. The aldehydes are Norrish I type products, requiring α cleavage of ketone **1** or **2**, and are clearly inaccessible in the photocycloaddition direction.

Kelly, Kelly, and McMurry[44] have studied the photocycloaddition of 3-phenyl-2-cyclohexenone and the 1-phenylpropene geometric isomers. They have discussed the role of biradicals in both cycloaddition and the concomitant geometric isomerization of 1-phenylpropene, concluding from triplet excitation energies that the geometric isomerization probably arises via the 1,4-biradical and is unlikely to involve excitation transfer. Our observation of ^{3}DPE demonstrates excitation transfer in the present case. The triplet excitation energies of 1-phenylpropene and DPE are similar,[45] but DMC has a triplet excitation energy substantially higher than that of 3-phenyl-2-cyclohexenone and thus is a better triplet excitation donor.[46] The energies in our case do in fact reasonably permit excitation transfer to DPE, so there is no anomaly. Kelly et al. also assigned an unidentified transient as either a triplet exciplex (by analogy to our earlier report[1]) or a triplet biradical analogous to those we consider here. The present results show that our previous study provides unreliable precedent for a triplet exciplex. Therefore, the unidentified transient is more likely a triplet biradical.

The presence of octahydrophenanthrenes **3** and **4** requires hydrogen transfer in each case. The mechanism for octahydrophenanthrene formation most reasonably involves triene intermediates, formed by 1,6 coupling of the biradicals, as shown in Figure 11. The 1,7-hydrogen shift would lead to rearomatization in a strongly exothermic process. Although there is no cogent direct evidence for the trienes, we note that their expected absorption in the 300−400 nm spectral region may well be the source of the permanent absorbance we observe in many of the temporal profiles.

Conclusion

A reaction mechanism for the photoaddition of DMC to DPE is presented in Figure 11. There are two initial interactions between ^{3}DMC and DPE: energy transfer and biradical formation. After the energy transfer, the ^{3}DPE thermally relaxes to ground-state DPE without chemical bond formation. The biradicals may revert to ground-state reactants or may undergo ring closure to form stable products. Two types of ring closure occur. The first is the 1,4-ring closure typical of this reaction; however, head-to-head cyclobutanes are not formed. The second type of annulation is an alpha−ortho closure resulting in unsaturated, substituted octahydrophenanthrenes. No regioselectivity is observed for the octahydrophenanthrenes, from which we conclude that ring closure is not problematic, as it appears to be in the 1,4-ring closure. We have concluded that multiple transient species are involved in this reaction. Among these transients ^{3}DPE is a major component. A prima facie case has been developed for the presence of the head-to-tail triplet state biradical. The evidence presented here does not forbid the existence of an exciplex intermediate. However, there is no basis in the transient data to invoke a triplet state exciplex.

Acknowledgment. This work was supported by the Robert A. Welch Foundation (Grant AT-0532) and the National Science Foundation (Grant CHE-9422824). We are indebted to Dr. Duane Hrncir for the X-ray crystallographic analysis of compounds **1** and **3**.

Supporting Information Available: Tables of positional and thermal parameters and complete bond distances and angles. Exerts of Excel spreadsheets showing data and cell formulas. This material is available free of charge via the Internet at http://pubs.acs.org.

References and Notes

(1) Caldwell, R. A.; Hrncir, D. C.; Munoz, T.; Unett, D. J. *J. Am. Chem. Soc.* **1996**, *118*, 8741.
(2) Schuster, D. I.; Lem, G.; Kaprindis, N. A. *Chem. Rev.* **1993**, *93*, 3.
(3) Corey, E. J.; Bass, J. D.; LeMahieu, R.; Mitra, R. B. *J. Am. Chem. Soc.* **1964**, *86*, 5570.
(4) Loutfy, R. O.; Yip, R. W.; Dogra, S. K. *Tetr. Lett.* **1977**, 2843.
(5) Loutfy, R. O.; de Mayo, P. J. *Am. Chem. Soc.* **1977**, *99*, 3559.
(6) Zachariasse, K. A.; Busse, R.; Schrader, U.; Kuhnle, W. *Chem. Phys. Lett.* **1982**, *89*, 303.
(7) Zachariasse, K. A. *Trends Photochem. Photobiol.* **1994**, *3*, 211.
(8) Subudhi, P. C.; Lim, E. C. *Chem. Phys. Lett.* **1978**, *58*, 62.
(9) Locke, R. J.; Lim, E. C. J. *Phys. Chem.* **1989**, *93*, 6017.
(10) Locke, R. J.; Lim, E. C. *Chem. Phys. Lett.* **1989**, *160*, 96.
(11) Caldwell, R. A. *J. Am. Chem. Soc.* **1970**, *92*, 1439.
(12) Caldwell, R. A. *J. Am. Chem. Soc.* **1973**, *95*, 1690.
(13) Caldwell, R. A.; Sovocool, G. W.; Gajewski, R. P. *J. Am. Chem. Soc.* **1973**, *95*, 2549.
(14) Kochevar, I. E.; Wagner, P. J. *J. Am. Chem. Soc.* **1972**, *94*, 3859.
(15) Maharaj, U.; Winnink, M. A. *J. Am. Chem. Soc.* **1981**, *103*, 2328.
(16) Wilson, T.; Halpern, A. M. *J. Am. Chem. Soc.* **1980**, *102*, 7279.
(17) Wilson, T.; Halpern, A. M. *J. Am. Chem. Soc.* **1981**, *103*, 2412.
(18) Jacques, P.; Allonas, X.; Von Raumer, M.; Suppan, P.; Haselbach, E. *J. Photochem. A: Chem.* **1997**, *111*, 41.
(19) Bauslaugh, P. G. *Synthesis* **1970**, 287.
(20) Schuster, D. I.; Heibel, G. E.; Brown, P. B.; Turro, N. J.; Kumar, C. V. *J. Am. Chem. Soc.* **1988**, *110*, 8261.
(21) Schuster, D. I. In *The Chemistry of Enones*; Patai, S., Rappoport, Z., Eds.; John Wiley and Sons Ltd: New York, 1989; pp 623−756.
(22) Schuster, D. I.; Heibel, G. E.; Woning, *J. Angew. Chem., Int. Ed. Engl.* **1991**, *30*, 1345.
(23) Schuster, D. I.; Lem, G.; Kaprindis, N. A. *Chem. Rev.* **1993**, *93*, 3.
(24) Freilich, S. C.; Peters, K. S. *J. Am. Chem. Soc.* **1981**, *103*, 6255.
(25) Freilich, S. C.; Peters, K. S. *J. Am. Chem. Soc.* **1985**, *107*, 3819.
(26) Andrew, D.; Hastings, D. J.; Weedon, A. C. *J. Am. Chem. Soc.* **1994**, *116*, 10870.
(27) Hastings, D. J.; Weedon, A. C. *J. Am. Chem. Soc.* **1991**, *113*, 8525.
(28) Maradyn, D. J.; Weedon, A. C. *Tetrahedron Lett.* **1994**, *35*, 8107.
(29) Rettig, T. A., Ph.D. Thesis, Iowa State University, Ames, Iowa, 1965.
(30) Our laboratory has observed this type of photoannulation with p-acetylstyrene and styrene, a tetralin was produced in low yield. See: Caldwell, R. A.; Diaz, J. F.; Hrncir, D. C.; Unett, D. J. *J. Am. Chem. Soc.* **1994**, *116*, 8138.
(31) Penn, J. H.; Orr, R. D. *J. Chem. Educ.* **1989**, *66*, 86.

(32) Caldwell, R. A. In *Kinetics and Spectroscopy of carbenes and Biradicals*; Platz, M. S., Ed.; Plenum Publishing Corp.: New York, 1990; pp 77−116.

(33) A temporal profile is a plot of optical density versus time of transient species.

(34) A time-resolved spectra are spectra collected at different times in the decay of a transient.

(35) Ni, T.; Caldwell, R. A.; Melton, L. A. *J. Am. Chem. Soc*. **1989**, *111*, 457.

(36) Milne-Thomson, L. M. *The Calculus of Finite Differences*.; Macmillan & Co. Ltd.: New York, 1960.

(37) For more information on the internal solution process used by Solver, contact: Frontline Systems, Inc. PO Box 4288 Incline Village, NV 89450-4288. Phone: (702) 831-0300.

(38) Silverstein, R. M.; Bassler, G. C.; Morril; T. C. *Spectrometric Identification Of Organic Compounds*, 4th ed.; John Wiley and Sons: New York, 1981; pp 15 and 208−233.

(39) Andrew, D.; Weedon, A. C. *J. Am. Chem. Soc*. **1995**, *117*, 5647−5663. Maradyn, D. J.; Weedon, A. C. *J. Am. Chem. Soc*. **1995**, *117*, 5359−5360.

(40) S_Δ and Φ_Δ refer to the fraction of oxygen quenching events leading to the production of singlet oxygen and the overall singlet oxygen quantum yield, respectively. The latter is simply the product of the quantum yield for formation of the triplet state being quenched by oxygen, Φ_T, and S_Δ. For more information, see: Gorman, A. A.; Rodgers, M. A. J. In *Handbook of Organic Photochemistry*; Scaiano, J. C., Ed.; CRC Press: Boca Raton, FL, 1989; pp 229−250.

(41) Unpublished result of Unett, D. J. ^{3}DPE generated by thioxanthone energy transfer is not quenched by the addition of azulene.

(42) Bader, M. *J. Chem. Educ*. **1980**, *57*, 703.

(43) Lowry, T. H.; Richardson, K. S. *Mechanism And Theory In Organic Chemistry*, 3rd ed.; Harper & Row Publishers: New York, 1987; pp 159−177.

(44) Kelly, J. F. D.; Kelly, J. M.; McMurry, T. B. H. *J. Chem. Soc., Perkin Trans. 2* **1999**, 1933−1941.

(45) Caldwell, R. A.; Ni Tuqiang, L. A.; Melton, *J. Am. Chem. Soc.* **1989**, *111*, 457−464.

(46) Caldwell, R. A.; Tang, W.; Schuster, D. I.; Heibel, G. E. *Photochem. Photobiol*. **1990**, *52*, 645−648.